

**Inhibitory effects of chalcone glycosides isolated from *Brassica rapa* L.
'hidabeni' and their synthetic derivatives on LPS-induced NO
production in microglia**

Hirokazu Hara,^{a,*} Yoko Nakamura,^a Masayuki Ninomiya,^b Ryosuke Mochizuki,^b

Tetsuro Kamiya,^a Elias Aizenman,^c Mamoru Koketsu,^b and Tetsuo Adachi^a

^a*Laboratory of Clinical Pharmaceutics, Gifu Pharmaceutical University, 1-25-4*

Daigaku-nishi, Gifu, 501-1196, Japan

^b*Department of Materials Science and Technology, Faculty of Engineering, Gifu*

University, 1-1 Yanagido, Gifu 501-1193, Japan

^c*Department of Neurobiology, University of Pittsburgh School of Medicine, Pittsburgh,*

PA 15261, USA

*Corresponding author:

Hirokazu Hara, Ph.D.

Laboratory of Clinical Pharmaceutics

Gifu Pharmaceutical University

1-25-4 Daigaku-nishi

Gifu, 501-1196, Japan

Phone: +81-58-230-8100

Fax: +81-58-230-8105

E-mail: harah@gifu-pu.ac.jp

Abbreviations

AlCl₃, aluminium chloride; Ag₂CO₃, silver carbonate; BF₃·Et₂O, boron trifluoride-etherate; CNS, central nervous system; CHCl₃, chloroform; CC, column chromatography; ESI, electrospray ionization; EtOAc, ethyl acetate; ERK, extracellular signal-regulated kinase; GAPDH, glyceraldehyde-3-phosphate dehydrogenase; iNOS, inducible NO synthase; IFN-β, interferon-β; IL-1β, interleukin-1β; LPS, lipopolysaccharide; JAK, Janus kinase; JNK, c-Jun N-terminal kinase; LC, liquid chromatography; L-NAME, N(G)-nitro-L-arginine methyl ester; MAPK, mitogen-activated protein kinase; NO, nitric oxide; NF-κB, nuclear factor kappa B; QTOF, quadrupole time of flight; STAT1, signal transduction and activator of transcription 1; TLR4, toll-like receptor 4; TNF-α, tumor necrosis factor-α.

ABSTRACT

Activation of microglia induces the production of various inflammatory mediators including nitric oxide (NO), leading to neurodegeneration in many central nervous system diseases. In this study, we examined the effects of chalcone glycosides isolated from *Brassica rapa* L. 'hidabeni' on lipopolysaccharide (LPS)-induced NO production using rat immortalized microglia HAPI cells.

4'-*O*- β -D-Glucopyranosyl-3',4-dimethoxychalcone (**A2**) inhibited LPS-induced inducible NO synthase (iNOS) expression and NO production. However, **A2** did not affect nuclear factor- κ B and mitogen-activated protein kinase pathways. The signal transduction and activator of transcription 1 (STAT1), which is activated via production of IFN- β by LPS, is an important transcription factor responsible for LPS-induced iNOS expression. **A2** suppressed LPS-induced phosphorylation and nuclear translocation of STAT1, although it had no effects on LPS-induced IFN- β expression. These results indicate that the inhibitory effect of **A2** is due to the prevention of STAT signaling. Moreover, structure-activity relationship studies on newly synthesized 'hidabeni' chalcone derivatives showed that 4'-*O*- β -D-glucopyranosyl-3'-methoxychalcone (**A11**), which has no functional groups in the B-ring, inhibits LPS-induced NO production more potently than **A2**.

Keywords: *Brassica rapa* L. 'hidabeni'; chalcone glycoside; microglia; inducible nitric oxide synthase; signal transduction and activator of transcription 1

1. Introduction

Microglia, resident immune cells in the central nervous system (CNS), are involved in the progression of neurodegeneration in many CNS disorders, such as ischemic stroke and Alzheimer's disease.^{1, 2} It has been reported that cerebral ischemia stimulates activation of microglia in the injured area and elicits a robust neuroinflammatory response.¹ Activated microglia produce inflammatory mediators including nitric oxide (NO). NO, which is a multifunctional effector molecule, is produced by inducible NO synthase (iNOS) in activated microglia. Increasing evidence suggests that the excess NO released from activated microglia results in neuronal cell death.^{3, 4}

Toll-like receptor 4 (TLR4) plays a key role in innate immunity. TLR4-mediated signaling stimulates expression of various inflammatory response genes including iNOS and proinflammatory cytokines, tumor necrosis factor- α (TNF- α) and interleukin-1 β (IL-1 β).⁵ Recent studies suggest that TLR4 signaling exacerbates ischemic outcomes.^{5, 6} For example, it was reported that a loss of function of TLR4 in TLR4 mutant mice protects against focal cerebral ischemia-induced neurodegeneration.⁷ Therefore, activation of TLR4 signaling caused by ischemic stroke is thought to be responsible for neuronal cell death associated with brain ischemia. Lipopolysaccharide (LPS), one of the major constituents of the outer membrane of Gram-negative bacteria, is a ligand of TLR4 and triggers expression of iNOS and proinflammatory cytokines through activation of TLR4. Nuclear factor kappa B (NF- κ B) and signal transduction and activator of transcription 1 (STAT1) have been shown to be key transcription factors responsible for LPS-induced iNOS expression.⁸

NF- κ B is sequestered in the cytoplasm by the inhibitory protein, inhibitor- κ B (I- κ B), under normal conditions. LPS promotes the degradation of I- κ B, and in turn

stimulates the translocation of NF- κ B to the nucleus.⁹ The binding site of NF- κ B is reported to be located in the regulatory region of *iNOS* gene.¹⁰ On the other hand, activation of STAT1 is mainly regulated via an autocrine loop involving interferon- β (IFN- β) produced by LPS-activated macrophages.^{11, 12} Secreted IFN- β stimulates phosphorylation of STAT1, and in turn promotes formation of STAT1 dimerization and its translocation to the nucleus. Since LPS-induced iNOS expression has been shown to be suppressed in macrophages prepared from *STAT1*^{-/-} mice,¹³ STAT1 is known to be indispensable for this phenomenon.

Chalcone, a subgroup of flavonoids, has been demonstrated to possess anti-inflammatory,¹⁴ anti-allergic¹⁵ and anti-oxidant¹⁶ activities. Recently, we reported that chalcone glycosides isolated from *Brassica rapa* L. 'hidabeni' have inhibitory effects on antigen-induced degranulation in basophilic leukemia RBL-2H3 cells.^{17, 18} In this study, we found that 'hidabeni' chalcones and their synthetic derivatives suppress LPS-induced iNOS expression and NO production in rat immortalized microglia, HAPI cells. Furthermore, we also addressed the mechanism underlying the inhibitory effects of these compounds on LPS-induced iNOS expression.

2. Results

2.1. Effects of compounds on LPS-induced iNOS expression

To confirm whether LPS induces iNOS expression under our conditions, HAPI cells were treated with 100 ng/mL LPS. As shown in Figure 1A, the induction of iNOS mRNA reached a peak at 6 h. LPS induced iNOS mRNA in a dose-dependent manner (Figure 1B). Next, to test the effects of compounds (**A1** – **A6**, Figure 2) on LPS-induced iNOS expression, we performed RT-PCR. HAPI cells were pretreated with each

compound (50 μ M) for 30 min, followed by the treatment with LPS (100 ng/mL). As shown in Figure 3A, **A2** reduced the expression of iNOS mRNA induced by LPS and other compounds had weak inhibitory activities. In addition, we examined the effect of these compounds on LPS-induced NO production. As shown in Figure 3B, treatment of HAPI cells with LPS promoted generation of NO. **A1** and **A2** significantly prevented LPS-induced NO production. These results indicated that **A2** most potently suppressed LPS-induced iNOS expression. Although we tested the effect of the compounds on LPS-induced IL-1 β expression, only **A2** had a weak, albeit significant, effect (Figure 3A).

2.2. Effect of **A2** on the NF- κ B and MAPK pathways

In the next step, we addressed the mechanism by which **A2** inhibits iNOS expression induced by LPS. It has been reported that LPS triggers iNOS expression via NF- κ B and mitogen-activated protein kinase (MAPK) pathways.^{8, 19} We investigated the effects of **A2** on the activation of both pathways caused by LPS. To determine whether **A2** inhibits translocation of NF- κ B induced by LPS, we performed Western blot analysis using nuclear extracts. As shown in Figure 4A, **A2** had no effects on the translocation of NF- κ B to the nucleus.

To investigate the effect of **A2** on the activation of MAPKs caused by LPS, we performed Western blot analysis for phosphorylation of ERK, JNK and p38 using cell lysates. As shown in Figure 4B, although ERK was constitutively phosphorylated in HAPI cells, phosphorylation of JNK and p38 was induced by the treatment with LPS. However, **A2** did not affect the phosphorylation state of MAPKs. These results indicate that **A2** suppressed LPS-induced iNOS expression independently of the NF- κ B and

MAPK pathways.

2.3. A2 suppressed IFN- β signal triggered by LPS

The production of IFN- β is up-regulated in response to LPS in macrophages. Secreted IFN- β binds to type I-IFN receptor, and in turn stimulates phosphorylation of STAT1 via the receptor-associated Janus kinase (JAK).²⁰ The JAK-STAT pathway has been shown to be responsible for LPS-induced iNOS expression.^{11, 13} To investigate the effect of the compounds on LPS-induced IFN- β mRNA expression in HAPI cells, we performed RT-PCR. HAPI cells were pretreated with each compound (50 μ M) for 30 min, followed by the treatment with LPS (100 ng/mL) for 6 h. However, as shown in Figure 5A, these compounds hardly affected LPS-induced IFN- β mRNA expression. Next, we examined the effect of **A2** on phosphorylation of STAT1 caused by LPS. As shown in Figure 5B, Western blot analysis revealed that LPS induced phosphorylation of STAT1 and **A2** suppressed the phosphorylation. Phosphorylation of STAT1 promotes translocation of STAT1 to the nucleus. Therefore, we examined the effect of **A2** on LPS-induced nuclear translocation of STAT1. As expected, **A2** suppressed translocation of STAT1 to the nucleus (Figure 5C).

2.4. Synthesis of chalcone glycoside derivatives

As a continuation to the above-mentioned studies, we were interested in the structure-activity relationships of chalcone glycoside derivatives with a focus on the B-ring structures against NO production. Comparative analyses with a variety of chalcone glycoside derivatives having different functional groups are necessary to examine the inhibitory effects of the most potent compounds.

Therefore, we synthesized a series of chalcone glycoside derivatives through the Claisen-Schmidt reaction of acetophenone **1** and benzaldehydes **2a-2g** using $\text{BF}_3 \cdot \text{Et}_2\text{O}$,²¹ followed by Koenigs-Knorr glycosylation (Scheme 1). Of the many methods available for the synthesis of chalcones, the most widely used is the base-catalyzed Claisen-Schmidt reaction. Although we first endeavored to prepare the chalcone using the NaOH aq method, the yield was quite low. Next, we tried to prepare the chalcone via acid-catalyzed methodologies using AlCl_3 or $\text{BF}_3 \cdot \text{Et}_2\text{O}$. Both conditions gave the chalcone, and we chose the $\text{BF}_3 \cdot \text{Et}_2\text{O}$ method, which produced the product in higher yield than the AlCl_3 method. Treatment of acetophenone **1** with 2 equiv. of benzaldehydes **2a-2g** was carried out in the presence of $\text{BF}_3 \cdot \text{Et}_2\text{O}$ (5 equiv.) in 1,4-dioxane for 19 h. The reaction was carried out successfully at room temperature, and the desired chalcones **3a-3g** were obtained after the usual workup of the reaction mixtures. For glycosylation, we first attempted to employ the Schmidt glycosylation conditions. However, the product was an α/β anomer mixture of the glucopyranose. Finally, chalcones were glycosylated using tetra-*O*-acetylglucopyranosyl bromide with Ag_2CO_3 as a promoter in pyridine. The acetyl groups of products **4a-4g** were deprotected with sodium methoxide to yield the corresponding chalcone glycoside derivatives **A1**, **A2** and **A7-A11**.

2.5. Structure-activity relationships of chalcone glycoside derivatives

We examined the effects of newly synthesized compounds on LPS-induced NO production and iNOS mRNA expression. As shown in Figure 6A, **A11** that has no functional groups in the B-ring potently inhibited NO production to an extent similar to that of the iNOS inhibitor, N(G)-nitro-L-arginine methyl ester (L-NAME). As expected,

it also suppressed iNOS mRNA induction caused by LPS (Figure 6B). As described above, **A2** that has one methoxy group at the 4-position of the B-ring had inhibitory effects, while **A1** having one hydroxy at the same position and other compounds having more than one hydroxy and/or methoxy groups at the 3-, 4- and/or 5-positions of the B-ring exerted weak or no effects.

3. Discussion

NO is thought to be an important mediator of progression of neurodegeneration in many CNS diseases. Excessive NO release under pathological conditions results in neuronal cell death. We have demonstrated here that **A2** from the aerial parts of *Brassica rapa* L. ‘hidabeni’ prevents LPS-induced iNOS expression and NO production in HAPI cells. In addition, we addressed the mechanism by which this compound suppresses LPS-induced iNOS expression, and found that it inhibits the activation of STAT1 caused by LPS.

Binding LPS to TLR4 elicits a variety of biological functions including the expression of pro-inflammatory gene products such as cytokines and iNOS. The NF- κ B and MAPK pathways have been shown to be critically involved in LPS-induced iNOS expression.^{8, 19} In fact, we also confirmed that the NF- κ B inhibitor, BAY11-7082, and the JNK inhibitor, SP600125, suppressed LPS-induced iNOS mRNA expression in HAPI cells (data not shown). Therefore, both pathways are thought to be involved, at least in part, in the induction of iNOS mRNA by LPS in HAPI cells. However, **A2** had no effects on LPS-induced nuclear translocation of NF- κ B and phosphorylation of JNK. Therefore, these pathways activated by LPS are unlikely to contribute to the inhibitory effect of **A2** on LPS-induced iNOS mRNA expression. In addition, we also found that

the inhibitory effect of **A2** on IL-1 β mRNA induction by LPS was weak compared with the inhibitory effect on iNOS mRNA induction. Because NF- κ B plays an important role in LPS-induced IL-1 β expression,²² this result concerning IL-1 β supports the finding that **A2** has only a weak inhibitory activity toward the NF- κ B pathway. On the other hand, it has been reported that the inhibitory effects of various chalcone derivatives on LPS-induced iNOS mRNA expression are due to their function of preventing LPS-induced NF- κ B and/or MAPK activation.^{16, 23-26} Therefore, these findings suggest that the differences between these chalcone derivatives and **A2** in terms of the mechanisms of action might be due to differences in chemical structures because the chalcones isolated from *B. rapa* L. 'hidabeni' have a unique structure.¹⁷

NF- κ B signaling alone is not sufficient to accomplish maximal induction of iNOS by LPS in macrophages. IFN- β that is secreted in response to LPS has been shown to be an essential mediator for iNOS induction.^{11, 12} For example, it was reported that neutralizing antibody against IFN- β attenuates induction of iNOS mRNA caused by LPS in macrophages.¹¹ However, **A2** failed to suppress the induction of IFN- β mRNA by LPS. Transcriptional regulation of *IFN- β* gene has been shown to be mediated via various signaling pathways. Several binding sites for transcription factors including NF- κ B and activator protein-1 (AP-1) are located in the regulatory region of *IFN- β* gene.²⁷ We also confirmed that the pharmacological inhibitor of NF- κ B or JNK, which is associated with AP-1 activation, reduced LPS-induced IFN- β mRNA expression in HAPI cells (data not shown). As described above, however, **A2** did not prevent LPS-induced activation of both NF- κ B and JNK pathways. Therefore, our finding that **A2** did not affect LPS-induced IFN- β mRNA expression seems reasonable.

Binding of secreted IFN- β to type I-IFN receptor stimulates the activation of

STAT1. It was reported that LPS-induced iNOS expression is markedly suppressed in macrophages prepared from *STAT1*^{-/-} mice.¹³ Therefore, STAT signal plays a key role in iNOS induction caused by LPS. We demonstrated here that **A2** prevents LPS-induced activation of STAT1 including phosphorylation and translocation to the nucleus. It has been reported that Tyr-701²⁸ and Ser-727^{28, 29} residues were identified as phosphorylation sites in STAT1. Phosphorylation of Tyr-701 results in dimerization and nuclear translocation of STAT1, whereas phosphorylation of Ser-727 is required for the augmentation of transcriptional ability of STAT1. In this study, we employed anti-phospho Tyr-701 antibody to detect the phosphorylation state of STAT1. Because JAK is responsible for the phosphorylation of Tyr-701, it is likely that **A2** inhibits JAK activation. Although ERK³⁰ or p38³¹ is reported to be involved in phosphorylation at Ser-727, **A2** had no inhibitory effects on activation of both kinases. Therefore, **A2** is unlikely to influence the phosphorylation of STAT1 at Ser-727 caused by LPS.

A number of chalcones have been reported to possess anti-inflammatory activities. As described above, the properties of these chalcones are attributable to the inhibitory activities toward the NF-κB and MAPK pathways.^{16, 23-26} However, **A2** hardly affected either of these signaling pathways. Because **A2** suppressed LPS-induced STAT1 activation, we speculate that it may inhibit activation of the JAK-STAT pathway. On the other hand, other tyrosine protein kinases such as c-Src have been reported to be involved in phosphorylation of STAT1.³² Moreover, it was also demonstrated that butein (2',3,4,4'-tetrahydroxychalcone) induces expression of the protein tyrosine phosphatase SHP-1 that is involved in the down-regulation of STAT1 phosphorylation.³³ Therefore, at present, we cannot rule out the possibility that kinases other than JAK or protein tyrosine phosphatases contribute to the inhibitory effect of **A2**.

On the basis of the structure of **A2**, we synthesized five new chalcone glycoside derivatives. Among compounds tested, compound **A11** that had no hydroxy and methoxy groups in the B-ring most potently inhibited LPS-induced NO production and iNOS mRNA expression. The addition of two or more functional groups to the B-ring reduced the inhibitory activities of the chalcone derivatives. It is probable that the mechanism of inhibitory activities of **A11** is similar to that of **A2**. Further studies are needed to identify target molecule(s) of **A2** and **A11**.

In conclusion, we demonstrated here that **A2**, a ‘hidabeni’ chalcone derivative, prevents LPS-induced NO production in immortalized microglia HAPI cells. The inhibitory effects of **A2** might be due to the suppression of LPS-induced STAT1 activation. Moreover, structure-activity relationship studies led to the identification of **A11**, which potently inhibited NO production and iNOS induction. Microglia play a key role in the progression of neurodegeneration in CNS disorders. We think that these compounds might be good candidates for the development of novel neuroprotective drugs.

4. Experimental section

4.1. Biochemical methods

4.1.1. Materials

LPS was purchased from Sigma (St. Louis, MO). Anti-STAT1, anti-phospho-JNK (Thr183/Thr185), anti-JNK, anti-phospho ERK, anti-ERK, anti-phospho p38 and anti-p38 antibodies were purchased from Cell Signaling Technology (Denver, MA). Anti-phospho-STAT1 (Thr701) antibody was purchased from Signalway Antibody (Pearland, TX). Anti-NF- κ B p65 antibody was purchased from Santa Cruz

Biotechnology (Santa Cruz, CA). Anti-actin antibody was purchased from Millipore (Billerica, MA). L-NAME was purchased from Wako Pure Chemical Industries (Osaka, Japan).

4.1.2. Cell culture

Rat immortalized-microglia HAPI cells were generously donated by Dr. J. Connor (Pennsylvania State University, Hershey, PA). HAPI cells were cultured in DMEM containing 10% heat-inactivated fetal calf serum (FCS), 4 mM glutamine, 100 units/mL penicillin G and 0.1 mg/mL streptomycin in a humidified 5% CO₂/95% air incubator at 37°C.

4.1.3. RT-PCR

HAPI cells were seeded in a 6-cm-diameter dish at a density of $\sim 7.0 \times 10^5$ cells in DMEM containing 1% FCS. The next day, cells were treated with LPS at various concentrations of LPS for the time indicated in the figure legends. Total RNA was extracted from the treated cells with TRIzol reagent (Invitrogen, Carlsbad, CA). First-strand cDNA was synthesized from 4 µg of total RNA. Aliquots of transcription reaction mixture (1 µL) were amplified with primers specific for rat iNOS (forward primer, 5'-TTGCTTCTGTGCTAATGCGG-3'; reverse primer, 5'-CAGAACTGAGGGTACATGCT-3'), IL-1β (forward primer, 5'-AGTGTCTGAAGCAGCTATGG-3'; reverse primer, 5'-TCATCATCCCACGAGTCACA-3'), IFN-β (forward primer, 5'-ATCGACTACAAGCAGCTCCA-3'; reverse primer, 5'-ACCTTTGTACCCTCCAGTAA-3') and glyceraldehyde-3-phosphate dehydrogenase

(GAPDH) (forward primer, 5'-ACCACAGTCCATGCCATCAC-3'; reverse primer, 5'-TCCACCACCCTGTTGCTGTA-3'). For amplification of iNOS, PCR was carried out using EX Taq (Takara Bio, Shiga, Japan) as follows: 2 min at 94°C, one cycle; 40 s at 94 °C, 40 s at 58°C, 1 min at 72°C, 27 cycles. For amplification of IFN- β , PCR was carried out as follows: 2 min at 94 °C, one cycle; 40 s at 94 °C, 40 s at 54 °C, 1 min at 72 °C, 35 cycles. For amplification of IL-1 β and GAPDH, PCR was carried out as follows: 2 min at 94 °C, one cycle; 40 s at 94 °C, 40 s at 58 °C, 1 min at 72 °C, 30 or 18 cycles, respectively. Aliquots of the PCR mixtures were separated on 2% agarose gel and stained with ethidium bromide. Densitometric analyses were performed using Multi Gauge (Fuji Film, Tokyo, Japan). The iNOS, IL-1 β and IFN- β mRNA levels were normalized relative to the GAPDH mRNA level in each sample.

4.1.4. Preparation of whole cell and nuclear extracts

After the treatment, the cells were washed twice with ice-cold PBS. For preparation of whole cell extracts, the cells were collected using 150 μ L of buffer A (20 mM Tris-HCl, pH 7.4, containing 1 mM EDTA, 1 mM EGTA, 1% Triton X-100, 10 mM NaF, 1 mM Na₃VO₄, 20 mM β -glycerophosphate, 5 μ g/mL leupeptin, 1 mM phenylmethylsulfonyl fluoride (PMSF) and 1 mM dithiothreitol (DTT)), and were lysed on ice for 30 min. The lysates were centrifuged at 14,000 rpm for 10 min at 4 °C to remove cellular debris. For preparation of nuclear extracts, the cells were collected using buffer B (20 mM HEPES-NaOH, pH 7.8, containing 15 mM KCl, 2 mM MgCl₂, 5 μ g/mL leupeptin, 0.5 mM PMSF and 2 mM DTT), and centrifuged. The cells were lysed in buffer C (buffer B containing 0.2% Nonidet P-40) for 5 min on ice, and centrifuged. Finally, the pellets were suspended in buffer D (20 mM HEPES-NaOH, pH

7.8, containing 0.4 M NaCl, 10% glycerol, 5 µg/mL leupeptin, 0.5 mM PMSF and 2 mM DTT), and stood for 30 min on ice. The nuclear extracts were centrifuged at 14,000 rpm for 10 min at 4 °C to remove cellular debris. The protein content of the supernatants was determined using Bio-Rad protein assay reagent.

4.1.5. Western blotting

Whole cell lysates (40 µg) or nuclear extracts (10 µg) were separated by SDS-PAGE on 10% or 12% (w/v) polyacrylamide gels. After being transferred onto a PVDF membrane, the blotted membrane was blocked using PBS containing 1% BSA. The membrane was incubated with each primary antibody (1:1,000), biotin-conjugated second antibody (1:2,000) and ABC reagents (Vector Laboratories, Inc., Burlingame, CA) (1:5,000), and then visualized using the Super-signal West Pico Chemiluminescent Substrate (Thermo Fisher Scientific Inc., Waltham, MA).

4.1.6. Measurement of nitrite production

HAPI cells were seeded in a 24-well plate at a density of $\sim 1.0 \times 10^5$ cells in DMEM containing 1% FCS. The next day, the cells were treated with 100 ng/mL LPS in the presence or absence of compounds for 24 h. The nitrite concentrations in the medium were measured using NO₂/NO₃ Assay Kit-C II (Dojin Chemicals, Kumamoto, Japan) according to the manufacturer's protocol.

4.1.7. Statistical analysis

Data were analyzed using ANOVA followed by *post hoc* Bonferroni tests or Student's t-test. A *P* value less than 0.05 was considered significant.

4.2. General Chemistry Methods

All solvents and reagents were purchased from the suppliers and used without further purification. IR spectra were recorded on a JASCO FT/IR-460 Plus spectrophotometer. ^1H (400 MHz) and ^{13}C (100 MHz) NMR spectra were recorded with a JEOL ECX 400 spectrometer with tetramethylsilane as an internal standard. MS spectra were obtained using a Waters XeroTM QTOFMS. Optical rotations were measured using a HORIBA SEPA-300 polarimeter at a specified temperature and concentration in the solvents indicated. Silica gel column chromatography (CC) was performed on silica gel N-60 (40–50 μm). Thin-layer chromatography (TLC) spots on plates pre-coated with silica gel 60 F₂₅₄ were detected with a UV lamp (254 nm). Fractionations for all CCs were based on TLC analyses.

4.3. Isolated Compounds from *Brassica rapa* L. ‘hidabeni’

The detailed isolation procedure was carried out as described previously. The spectral data of isolated compounds **A1–A6** have been mentioned in the literature.^{17, 18}

4.4. Synthesis of chalcones **3a–3g**

Boron trifluoride-etherate (6.0 mmol) was added to a stirred solution of 4'-hydroxy-3'-methoxyacetophenone **1** (1.2 mmol) and benzaldehydes **2a–2g** (2.4 mmol) in 1,4-dioxane (10 mL) at room temperature. After stirring for 19 h, the resultant solution was partitioned with EtOAc, washed with 10% HCl aq, distilled water, brine, dried over anhydrous Na₂SO₄ and concentrated in vacuo. The residue was purified using silica gel CC eluted with *n*-hexane/CHCl₃ (2/1) to yield chalcones **3a–3g**.

4.4.1. 4-O-Acetyl-4'-hydroxy-3'-methoxychalcone (3a)

Yellow powder, 40% yield. IR (film): 3372, 1653, 1590 cm^{-1} . ^1H NMR (400 MHz, $(\text{CD}_3)_2\text{CO}$): δ 7.87 (1H, d, J = 15.6 Hz, H- β), 7.86 (2H, m, H-2 and H-6), 7.80 (1H, dd, J = 8.2, 2.3 Hz, H-6'), 7.75 (1H, d, J = 15.6 Hz, H- α), 7.70 (1H, s, H-2'), 7.21 (2H, d, J = 9.2 Hz, H-3 and H-5), 6.97 (1H, d, J = 8.2 Hz, H-5'), 3.94 (3H, s, 3'-OMe), 2.28 (3H, s, 4-OAc). ^{13}C NMR (100 MHz, $(\text{CD}_3)_2\text{CO}$): δ 187.8, 169.5, 153.3, 152.4, 148.5, 142.6, 133.8, 131.4, 130.4, 124.4, 123.2, 122.9, 115.4, 112.1, 56.3, 20.9.

4.4.2. 3',4-Dimethoxy-4'-hydroxychalcone (3b)

Yellow powder, 58% yield. IR (film): 3403, 1645, 1593 cm^{-1} . ^1H NMR (400 MHz, CDCl_3): δ 7.78 (1H, d, J = 15.8 Hz, H- β), 7.65-7.63 (2H, m, H-2' and H-6'), 7.59 (2H, d, J = 8.7 Hz, H-2 and H-6), 7.43 (1H, d, J = 15.8 Hz, H- α), 6.99 (1H, d, J = 8.2 Hz, H-5'), 6.93 (2H, d, J = 8.7 Hz, H-3 and H-5), 3.84 (3H, s, 3'-OMe), 3.95 (3H, s, 4-OMe). ^{13}C NMR (100 MHz, CDCl_3): δ 188.6, 161.5, 150.2, 146.8, 143.8, 131.1, 130.0, 127.7, 123.5, 119.2, 114.3, 113.8, 110.5, 56.0, 55.3.

4.4.3. 4'-Hydroxy-3,3',4-trimethoxychalcone (3c)

Yellow powder, 65% yield. IR (film): 3404, 1645, 1587 cm^{-1} . ^1H NMR (400 MHz, $(\text{CD}_3)_2\text{CO}$): δ 8.48 (1H, bs), 7.81-7.66 (3H, m, H-2', H-6', H- α , and H- β), 7.48 (1H, d, J = 1.8 Hz, H-2), 7.34 (1H, dd, J = 8.6, 2.3 Hz, H-6), 7.02 (1H, d, J = 8.1 Hz, H-5'), 6.94 (1H, d, J = 8.1 Hz, H-5), 3.94 (3H, s, 3'-OMe), 3.90 (3H, s, 3-OMe), 3.87 (3H, s, 4-OMe). ^{13}C NMR (100 MHz, $(\text{CD}_3)_2\text{CO}$): δ 187.1, 151.8, 151.4, 149.8, 147.7, 143.3, 128.3, 123.4, 123.2, 119.6, 114.5, 111.6, 111.2, 110.8, 55.5, 55.4.

4.4.4. 4'-Hydroxy-3,3',4,5-tetramethoxychalcone (3d)

Yellow powder, 39% yield. IR (film): 3371, 1654, 1587 cm^{-1} . ^1H NMR (400 MHz, $(\text{CD}_3)_2\text{CO}$): δ 7.81 (1H, d, $J = 15.6$ Hz, H- β), 7.76 (1H, dd, $J = 8.2, 3.2$ Hz, H-6'), 7.69 (1H, d, $J = 15.6$ Hz, H- α), 7.67 (1H, d, $J = 3.2$ Hz, H-2'), 7.16 (2H, s, H-2 and H-6), 6.95 (1H, d, $J = 8.5$ Hz, H-5'), 3.94 (3H, s, 3'-OMe), 3.91 (6H, s, 3-OMe and 5-OMe), 3.78 (3H, s, 4-OMe). ^{13}C NMR (100 MHz, $(\text{CD}_3)_2\text{CO}$): δ 187.9, 154.6, 152.3, 148.6, 144.1, 141.3, 131.7, 131.6, 124.3, 122.0, 115.3, 112.0, 107.0, 60.6, 56.6, 56.3.

4.4.5. 4-O-Acetyl-4'-hydroxy-3,3',5-trimethoxychalcone (3e)

Yellow powder, 50% yield. IR (film): 3392, 1645, 1593 cm^{-1} . ^1H NMR (400 MHz, $(\text{CD}_3)_2\text{CO}$): δ 7.89 (1H, d, $J = 15.8$ Hz, H- β), 7.77 (1H, dd, $J = 8.3, 1.8$ Hz, H-6'), 7.71 (1H, d, $J = 15.8$ Hz, H- α), 7.68 (1H, d, $J = 1.8$ Hz, H-2'), 7.22 (2H, s, H-2 and H-6), 6.95 (1H, d, $J = 8.2$ Hz, H-5'), 3.94 (3H, s, 3'-OMe), 3.90 (6H, s, H-3 and H-5), 2.81 (1H, bs), 2.26 (3H, s, 4-OAc). ^{13}C NMR (100 MHz, $(\text{CD}_3)_2\text{CO}$): δ 187.1, 167.6, 152.7, 151.6, 147.8, 142.8, 133.7, 130.6, 123.6, 122.2, 114.6, 111.2, 105.3, 55.8, 55.5, 19.4.

4.4.6. 3-O-Acetyl-3',4-dimethoxy-4'-hydroxychalcone (3f)

Yellow powder, 50% yield. IR (film): 3392, 1650, 1592 cm^{-1} . ^1H NMR (400 MHz, $(\text{CD}_3)_2\text{CO}$): δ 7.88 (1H, d, $J = 15.6$ Hz, H- β), 7.79 (1H, dd, $J = 8.2, 1.8$ Hz, H-6'), 7.74 (1H, d, $J = 15.6$ Hz, H- α), 7.69 (1H, d, $J = 1.8$ Hz, H-2'), 7.59 (1H, d, $J = 1.8$ Hz, H-2), 7.41 (1H, dd, $J = 8.2, 1.8$ Hz, H-6), 7.13 (1H, d, $J = 8.2$ Hz, H-5'), 6.95 (1H, d, $J = 8.2$ Hz, H-5), 3.95 (3H, s, 3'-OMe), 3.92 (3H, s, 4-OMe), 2.27 (3H, s, 3-OAc). ^{13}C NMR (100 MHz, $(\text{CD}_3)_2\text{CO}$): δ 187.0, 168.0, 151.8, 151.6, 147.5, 142.3, 141.2, 134.3, 130.9, 123.6, 123.3, 122.2, 121.5, 114.6, 112.1, 111.2, 55.6, 55.5, 19.9.

4.4.7. 4'-Hydroxy-3'-methoxychalcone (3g)

Yellow powder, 47% yield. IR (film): 3367, 1651, 1584 cm^{-1} . ^1H NMR (400 MHz, $(\text{CD}_3)_2\text{CO}$): δ 7.89 (1H, d, $J = 14.0$ Hz, H- β), 7.86-7.69 (3H, m, H-2', H-6', and H- α), 7.46-7.43 (3H, m, H-3, H-4, and H-5), 7.25-7.24 (1H, m, H-5'), 6.97 (2H, d, $J = 8.2$ Hz, H-2 and H-6), 3.95 (3H, s, 3'-OMe). ^{13}C NMR (100 MHz, $(\text{CD}_3)_2\text{CO}$): δ 188.1, 152.4, 148.5, 143.7, 136.1, 131.3, 130.9, 129.6, 129.2, 124.4, 122.7, 115.4, 112.0, 56.3.

4.5. Synthesis of acetylated chalcone glycosides 4a-4g

Silver carbonate (2.57 mmol) was added to a stirred solution of tetra-*O*-acetylglucopyranosyl bromide (1.45 mmol) and chalcones **3a-3g** (0.65 mmol) in pyridine (10 mL) at room temperature under shaded conditions. After stirring for 18 h, the resultant solution was partitioned with EtOAc, washed with 5 % HCl aq, distilled water, brine, dried over anhydrous Na_2SO_4 and concentrated in vacuo. The residue was purified using silica gel CC eluted with *n*-hexane/ CHCl_3 (1/1) to yield acetylated chalcone glycosides **4a-4g**.

4.5.1.

4'-(2,3,4,6-Tetra-*O*-acetyl- β -D-glucopyranosyl)-4-*O*-acetyl-3'-methoxychalcone (4a)

Yellow powder, 32% yield. IR (film): 3372, 1650, 1593 cm^{-1} . ^1H NMR (400 MHz, $(\text{CD}_3)_2\text{CO}$): δ 7.79-7.72 (2H, m, H-6' and H- β), 7.71-7.68 (3H, m, H-2, H-6, and H- α), 7.65 (1H, s, H-2'), 7.32 (1H, d, $J = 8.7$ Hz, H-5'), 6.92 (2H, d, $J = 8.7$ Hz, H-3 and H-5), 5.45 (1H, d, $J = 7.8$ Hz, H-1''), 5.40 (1H, t, $J = 9.6$ Hz, H-4''), 5.27-5.23 (1H, m, H-3''), 5.15 (1H, t, $J = 9.6$ Hz, H-2''), 4.34-4.29 (1H, m, H-5''), 4.22-4.17 (2H, m, H-6 α '' and

H-6 β "), 3.92 (3H, s, 3'-OMe), 2.15 (3H, s, 4-OAc), 2.05-1.97 (12H, m, 2''-OAc, 3''-OAc, 4''-OAc, and 6''-OAc). ^{13}C NMR (100 MHz, $(\text{CD}_3)_2\text{CO}$): δ 188.4, 170.6, 170.3, 170.0, 169.6, 160.8, 151.2, 150.9, 144.8, 135.3, 131.5, 127.6, 122.9, 119.5, 118.1, 116.7, 113.2, 100.1, 73.2, 72.7, 71.9, 69.2, 62.7, 56.6, 20.6.

4.5.2. 4'-(2,3,4,6-Tetra-O-acetyl- β -D-glucopyranosyl)-3',4-dimethoxychalcone (4b)

Yellow powder, 90% yield. IR (film): 1753, 1655, 1595 cm^{-1} . ^1H NMR (400 MHz, CD_3OD): δ 7.65 (1H, d, J = 16.0 Hz, H- β), 7.59 (2H, d, J = 8.7 Hz, H-2 and H-6), 7.54-7.47 (3H, m, H-2', H-6', and H- α), 7.16 (1H, d, J = 8.7 Hz, H-5'), 6.90 (2H, d, J = 8.7 Hz, H-3 and H-5), 5.32 (1H, d, J = 9.6 Hz, H-1''), 5.16 (1H, t, J = 11.0 Hz, H-3''), 5.04 (1H, t, J = 9.6 Hz, H-2''), 4.24 (1H, dd, J = 11.0, 5.5 Hz, H-6 α '), 4.13-4.09 (1H, m, H-6 β '), 3.98-3.93 (1H, m, H-5''), 3.80 (3H, s, 3'-OMe), 3.77 (3H, s, 4-OMe), 2.04-1.96 (12H, m, 2''-OAc, 3''-OAc, 4''-OAc, and 6''-OAc). ^{13}C NMR (100 MHz, CD_3OD): δ 189.1, 171.0, 170.3, 170.0, 169.8, 162.0, 150.2, 150.1, 144.6, 133.9, 130.4, 127.5, 122.4, 118.7, 116.8, 114.2, 112.0, 99.2, 72.6, 71.8, 71.2, 68.4, 61.8, 55.4, 54.7, 19.4, 19.3.

4.5.3. 4'-(2,3,4,6-Tetra-O-acetyl- β -D-glucopyranosyl)-3,3',4-trimethoxychalcone (4c)

Yellow powder, 85% yield. IR (film): 3373, 1755, 1643, 1592 cm^{-1} . ^1H NMR (400 MHz, CD_3OD): δ 7.72-7.68 (2H, m, H-6' and H- β), 7.60 (1H, d, J = 4.6 Hz, H-2'), 7.57 (1H, d, J = 15.6 Hz, H- α), 7.32 (1H, s, H-2), 7.25 (1H, dd, J = 8.2, 1.8 Hz, H-6), 7.19 (1H, d, J = 8.7 Hz, H-5'), 6.95 (1H, d, J = 8.7 Hz, H-5), 5.36 (1H, t, J = 9.6 Hz, H-3''), 5.26 (1H, d, J = 8.2 Hz, H-1''), 5.20 (1H, t, J = 9.6 Hz, H-2''), 5.09 (1H, t, J = 9.6 Hz,

H-4''), 4.29 (1H, dd, $J = 12.8, 5.0$ Hz, H-6 α ''), 4.15 (1H, dd, $J = 12.4, 4.9$ Hz, H-6 β ''), 4.02-3.99 (1H, m, H-5''), 3.88 (3H, s, 3'-OMe), 3.85 (6H, s, 3-OMe and 4-OMe), 2.15-1.99 (12H, m, 2''-OAc, 3''-OAc, 4''-OAc, and 6''-OAc). ^{13}C NMR (100 MHz, CD_3OD): δ 189.2, 170.9, 170.2, 169.9, 151.8, 150.2, 149.4, 145.0, 134.0, 128.0, 123.5, 122.4, 119.0, 116.9, 112.1, 111.2, 110.7, 99.2, 72.6, 71.8, 71.2, 68.3, 61.7, 55.4, 55.2, 55.1, 19.4, 19.3.

4.5.4.

4'-(2,3,4,6-Tetra-O-acetyl- β -D-glucopyranosyl)-3,3',4,5-tetramethoxychalcone (4d)

Yellow powder, 76% yield. IR (film): 3392, 1751, 1663, 1583 cm^{-1} . ^1H NMR (400 MHz, $(\text{CD}_3)_2\text{CO}$): δ 7.82-7.76 (2H, m, H-6' and H- β), 7.70 (1H, d, $J = 14.2$ Hz, H- α), 7.69 (1H, s, H-2'), 7.32 (1H, d, $J = 8.7$ Hz, H-5'), 7.17 (2H, s, H-2 and H-6), 5.47 (1H, d, $J = 8.2$ Hz, H-1''), 5.41 (1H, t, $J = 9.6$ Hz, H-3''), 5.26 (1H, t, $J = 7.8$ Hz, H-2''), 5.16 (1H, t, $J = 9.6$ Hz, H-4''), 4.31 (1H, dd, $J = 12.8, 5.5$ Hz, H-6 α ''), 4.22-4.18 (1H, m, H-6 β ''), 3.92 (3H, s, 3'-OMe), 3.91 (9H, s, 3-OMe, 4-OMe, and 5-OMe), 2.04 (12H, m, 2''-OAc, 3''-OAc, 4''-OAc, and 6''-OAc). ^{13}C NMR (100 MHz, $(\text{CD}_3)_2\text{CO}$): δ 187.6, 169.9, 169.5, 169.2, 168.7, 153.8, 150.4, 150.3, 144.1, 140.6, 134.2, 130.7, 122.3, 121.0, 117.2, 112.4, 106.3, 99.2, 72.3, 71.9, 71.0, 68.4, 61.8, 59.9, 55.8, 55.7, 19.8, 19.8, 19.7.

4.5.5.

4'-(2,3,4,6-Tetra-O-acetyl- β -D-glucopyranosyl)-4-O-acetyl-3,3',5-trimethoxychalcone (4e)

Yellow powder, 56% yield. IR (film): 3371, 1756, 1646, 1594 cm^{-1} . ^1H NMR (400 MHz, $(\text{CD}_3)_2\text{CO}$): δ 7.85 (1H, d, $J = 16.0$ Hz, H- β), 7.79 (1H, dd, $J = 8.7, 1.8$ Hz, H-6'),

7.73 (1H, d, $J = 16.0$ Hz, H- α), 7.69 (1H, d, $J = 1.8$ Hz, H-2'), 7.33 (1H, d, $J = 8.7$ Hz, H-5'), 7.22 (2H, s, H-2 and H-6), 5.47 (1H, d, $J = 8.2$ Hz, H-1''), 5.39 (1H, t, $J = 9.6$ Hz, H-3''), 5.25 (1H, dd, $J = 9.6, 8.0$ Hz, H-2''), 5.16 (1H, t, $J = 9.6$ Hz, H-4''), 4.31-4.98 (1H, m, H-6 α ''), 4.21-4.17 (2H, m, H-5'' and H-6 β ''), 3.92 (3H, s, 3'-OMe), 3.89 (6H, s, 3-OMe and 5-OMe), 2.2-1.99 (12H, m, 2''-OAc, 3''-OAc, 4''-OAc, and 6''-OAc). ^{13}C NMR (100 MHz, $(\text{CD}_3)_2\text{CO}$): δ 187.7, 169.9, 169.5, 169.2, 168.8, 167.8, 152.7, 150.4, 143.6, 134.1, 133.5, 130.7, 122.4, 122.2, 117.2, 112.4, 105.4, 99.2, 72.3, 72.0, 71.0, 68.4, 61.8, 55.8, 19.83, 19.78, 19.73, 19.5.

4.5.6.

4'-(2,3,4,6-Tetra-O-acetyl- β -D-glucopyranosyl)-3-O-acetyl-3',4-dimethoxychalcone (4f)

Yellow powder, 53% yield. IR (film): 3372, 1776, 1644, 1595 cm^{-1} . ^1H NMR (400 MHz, $(\text{CD}_3)_2\text{CO}$): δ 8.05-7.09 (7H, m, H-2, H-2', H-5', H-6, H-6', H- α , and H- β), 5.44-5.15 (4H, m, H-1'', H-3'', H-2'', and H-4''), 4.43-4.02 (3H, m, H-5'', H-6 α '', and H-6 β ''), 3.91 (6H, s, 3'-OMe and 4-OMe), 2.18-1.99 (12H, m, 2''-OAc, 3''-OAc, 4''-OAc, and 6''-OAc). ^{13}C NMR (100 MHz, $(\text{CD}_3)_2\text{CO}$): δ 187.6, 169.9, 169.6, 169.3, 168.9, 168.1, 151.8, 150.4, 143.2, 141.9, 134.0, 133.9, 123.4, 122.4, 122.0, 121.6, 117.2, 112.4, 112.2, 99.2, 72.4, 72.0, 71.0, 68.4, 61.9, 55.8, 55.6, 19.8.

4.5.7. 4'-(2,3,4,6-Tetra-O-acetyl- β -D-glucopyranosyl)-3'-methoxychalcone (4g).

Yellow powder, 47% yield. IR (film): 3404, 1754, 1649, 1587 cm^{-1} . ^1H NMR (400 MHz, $(\text{CD}_3)_2\text{CO}$): δ 7.88 (1H, d, $J = 16.0$ Hz, H- β), 7.84-7.76 (2H, m, H-6' and H- α), 7.73 (1H, d, $J = 1.9$ Hz, H-2'), 7.47-7.45 (4H, m, H-3, H-4, H-5, and H-5'), 7.34 (2H, d, $J =$

8.7 Hz, H-2 and H-6), 5.48 (1H, d, $J = 7.8$ Hz, H-1''), 5.41 (1H, t, $J = 9.6$ Hz, H-3''), 5.29-5.23 (1H, m, H-2''), 5.16 (1H, t, $J = 9.6$ Hz, H-4''), 4.33-4.26 (1H, m, H-6 α ''), 4.23-4.18 (2H, m, H-5'', and H-6 β ''), 3.93 (3H, s, 3'-OMe), 2.04-1.98 (12H, m, 2''-OAc, 3''-OAc, 4''-OAc, and 6''-OAc). ^{13}C NMR (100 MHz, $(\text{CD}_3)_2\text{CO}$): δ 187.6, 169.9, 169.5, 169.3, 168.9, 150.4, 143.7, 135.3, 134.0, 130.5, 129.4, 129.0, 128.7, 128.3, 122.4, 121.9, 117.2, 117.0, 112.4, 112.2, 99.2, 72.4, 72.0, 71.1, 68.4, 61.9, 55.8, 19.9, 19.81, 19.76.

4.6. Synthesis of chalcone glycosides **A1**, **A2** and **A7-A11**

Acetylated chalcone glycosides **4a-4g** were stirred in 10 mg/ml sodium methoxide/methanol solution (10 ml) for 10 minutes. The reaction mixture was neutralized using a Dowex Marathon C (H^+ form), filtrated and concentrated in vacuo. The residue was purified using silica gel CC eluted with $\text{CHCl}_3/\text{MeOH}$ (10/1) to yield chalcone glycosides **A1**, **A2** and **A7-A11**.

4.6.1. 4'-O- β -D-Glucopyranosyl-3,3',4-trimethoxychalcone (**A7**)

Yellow powder, Quantitative. $[\alpha]_{589}^{21} -25.0$ (c 0.10, MeOH). IR (film): 3404, 1647, 1587, 1512 cm^{-1} . ^1H NMR (400 MHz, $(\text{CD}_3)_2\text{CO}$): δ 7.79-7.76 (2H, m, H-6' and H- β), 7.73 (1H, d, $J = 16.3$ Hz, H- α), 7.67 (1H, d, $J = 2.1$ Hz, H-2'), 7.49 (1H, d, $J = 2.1$ Hz, H-5'), 7.34 (1H, dd, $J = 8.9$, 2.1 Hz, H-6'), 7.25 (1H, d, $J = 8.7$ Hz, H-2), 7.02 (1H, d, $J = 8.9$ Hz, H-5), 5.13 (1H, d, $J = 7.3$ Hz, H-1''), 3.92 (3H, s, 3'-OMe), 3.90 (1H, s, 3-OMe), 3.87 (1H, s, 4-OMe), 3.85-3.69 (3H, m, H-2'', H-6 α '', and H-6 β ''), 3.61-3.49 (3H, m, H-3'', H-4'', and H-5''). ^{13}C NMR (100 MHz, $(\text{CD}_3)_2\text{CO}$): δ 187.4, 151.0, 149.7, 149.6, 143.8, 132.8, 128.2, 123.5, 122.6, 119.4, 114.9, 111.8, 111.5, 110.7, 100.6, 77.2, 73.7, 70.3, 61.7, 55.6, 55.4, 55.3. LCESI-QTOFMS: m/z 499.1560 $[\text{M}+\text{Na}]^+$ (calcd. for

C₂₄H₂₈O₁₀Na, 499.1580).

4.6.2. 4'-O- β -D-Glucopyranosyl-3,3',4,5-tetramethoxychalcone (A8)

Yellow powder, 83% yield. $[\alpha]_{589}^{21}$ -10.0 (*c* 0.10, MeOH). IR (film): 3391, 1640, 1586 cm⁻¹. ¹H NMR (400 MHz, CD₃OD): δ 7.80 (1H, dd, *J* = 1.8 Hz, H-6'), 7.70-7.65 (1H, m, H-2', H- α , and H- β), 7.24 (1H, d, *J* = 8.7 Hz, H-5'), 7.05 (2H, s, H-2 and H-6), 5.06 (1H, d, *J* = 7.8 Hz, H-1''), 3.92 (3H, s, 3'-OMe), 3.90 (9H, s, 3-OMe, 4-OMe, and 5-OMe), 3.83-3.78 (3H, m, H-2'', H-6 α '', and H-6 β ''), 3.15-3.48 (2H, m, H-3'' and H-5''), 3.31 (1H, t, *J* = 1.4 Hz, H-4''). ¹³C NMR (100 MHz, CD₃OD): δ 189.3, 153.5, 151.1, 149.1, 144.6, 140.1, 132.4, 130.9, 123.2, 120.7, 114.7, 111.5, 105.9, 103.6, 100.5, 77.0, 76.5, 73.4, 69.9, 61.1, 59.9, 55.4, 54.7. LCESI-QTOFMS: *m/z* 507.1850 [M+H]⁺ (calcd. for C₂₅H₃₁O₁₁, 507.1866).

4.6.3. 4'-O- β -D-Glucopyranosyl-4-hydroxy-3,3',5-trimethoxychalcone (A9)

Yellow powder, Quantitative. $[\alpha]_{589}^{21}$ -10.0 (*c* 0.10, MeOH). IR (film): 3372, 1649, 1512 cm⁻¹. ¹H NMR (400 MHz, CD₃OD): δ 7.77 (1H, dd, *J* = 8.7, 1.8 Hz, H-6'), 7.69 (1H, d, *J* = 15.6 Hz, H- β), 7.64 (1H, d, *J* = 1.8 Hz, H-2'), 7.60 (1H, d, *J* = 15.6 Hz, H- α), 7.22 (1H, d, *J* = 8.7 Hz, H-5'), 7.03 (2H, s, H-2 and H-6), 5.06 (1H, d, *J* = 7.4 Hz, H-1''), 3.92 (3H, s, 3'-OMe), 3.90 (6H, s, 3-OMe and 5-OMe), 3.73-3.69 (2H, m, H-2'' and H-6 α ''), 3.56-3.42 (3H, m, H-3'', H-5'', and H-6 β ''), 3.30 (1H, t, *J* = 1.4 Hz, H-4'). ¹³C NMR (100 MHz, CD₃OD): δ 189.4, 150.9, 149.3, 148.1, 145.6, 138.9, 132.6, 125.9, 123.0, 118.5, 114.7, 111.5, 106.1, 100.5, 77.0, 76.5, 73.4, 69.9, 61.1, 55.5, 55.3. LCESI-QTOFMS: *m/z* 515.1514 [M+Na]⁺ (calcd. for C₂₄H₂₈O₁₁Na, 515.1529).

4.6.4. 4'-O- β -D-Glucopyranosyl-3',4-dimethoxy-3-hydroxychalcone (A10)

Yellow powder, 84% yield. $[\alpha]_{589}^{22}$ -15.0 (*c* 0.10, MeOH). IR (film): 3372, 1644, 1593, 1512 cm^{-1} . ^1H NMR (400 MHz, CD_3OD): δ 7.77 (1H, dd, J = 8.7, 1.8 Hz, H-6''), 7.72 (1H, d, J = 16.0 Hz, H- β), 7.66 (1H, d, J = 1.8 Hz, H-2'), 7.61 (1H, d, J = 16.0 Hz, H- α), 7.35 (1H, d, J = 1.8 Hz, H-2), 7.26 (1H, d, J = 8.7 Hz, H-5), 7.22 (1H, dd, J = 8.7, 1.8 Hz, H-6), 6.84 (1H, d, J = 8.2 Hz, H-5), 5.06 (1H, d, J = 7.3 Hz, H-1''), 3.93 (3H, s, 3'-OMe), 3.92-3.88 (1H, m, H-6 α ''), 3.71-3.68 (1H, m, H-6 β ''), 3.59-3.48 (3H, m, H-2'', H-3'', and H-5''), 3.31 (1H, t, J = 1.8 Hz, H-4''). ^{13}C NMR (100 MHz, CD_3OD): δ 189.5, 150.9, 149.7, 149.4, 148.1, 145.4, 132.7, 127.0, 123.6, 122.9, 118.2, 115.2, 114.8, 111.5, 110.9, 100.5, 77.0, 76.5, 73.4, 69.9, 61.1, 55.3, 55.2. LCESI-QTOFMS: m/z 485.1408 $[\text{M}+\text{Na}]^+$ (calcd. for $\text{C}_{23}\text{H}_{26}\text{O}_{10}\text{Na}$, 485.1424).

4.6.5. 4'-O- β -D-Glucopyranosyl-3'-methoxychalcone (A11)

Yellow powder, 92% yield. $[\alpha]_{589}^{22}$ -75.0 (*c* 0.10, MeOH). IR (film): 3373, 1666, 1599, 1511 cm^{-1} . ^1H NMR (400 MHz, CD_3OD): δ 7.80-7.74 (5H, m, H-2, H-6, H-6', H- α , and H- β), 7.68 (1H, d, J = 2.3 Hz, H-2'), 7.45-7.42 (3H, m, H-3, H-4, and H-5), 7.27 (1H, d, J = 8.7 Hz, H-5'), 5.07 (1H, d, J = 7.8 Hz, H-1''), 3.94 (3H, s, 3'-OMe), 3.86 (1H, dd, J = 12.4, 2.5 Hz, H-6 α ''), 3.69 (1H, dd, J = 12.4, 6.9 Hz, H-6 β ''), 3.56 (1H, t, J = 7.8 Hz, H-2''), 3.52-3.39 (2H, m H-3'' and H-5''), 3.30 (1H, t, J = 8.9 Hz, H-4''). ^{13}C NMR (100 MHz, CD_3OD): δ 189.3, 151.1, 149.5, 144.4, 135.0, 130.3, 128.7, 128.4, 128.0, 123.1, 121.3, 114.8, 111.4, 100.5, 77.0, 76.5, 73.4, 69.9, 61.1, 55.3. LCESI-QTOFMS: m/z 439.1357 $[\text{M}+\text{Na}]^+$ (calcd. for $\text{C}_{22}\text{H}_{24}\text{O}_8\text{Na}$, 439.1369).

Acknowledgment

This work was supported by a Grant-in-Aid for Scientific Research (C) from the Japan Society for the Promotion of Science (20590543 to H.H.).

References and notes

1. Weinstein, J. R.; Koerner, I. P.; Moller, T. *Future Neurol.* **2010**, *5*, 227.
2. Cameron, B.; Landreth, G. E. *Neurobiol. Dis.* **2010**, *37*, 503.
3. Knoch, M. E.; Hartnett, K. A.; Hara, H.; Kandler, K.; Aizenman, E. *Glia* **2008**, *56*, 89.
4. Bal-Price, A.; Brown, G. C. *J. Neurosci.* **2001**, *21*, 6480.
5. Buchanan, M. M.; Hutchinson, M.; Watkins, L. R.; Yin, H. *J. Neurochem.* **2010**, *114*, 13.
6. Hyakkoku, K.; Hamanaka, J.; Tsuruma, K.; Shimazawa, M.; Tanaka, H.; Uematsu, S.; Akira, S.; Inagaki, N.; Nagai, H.; Hara, H. *Neuroscience* **2010**, *171*, 258.
7. Tang, S. C.; Arumugam, T. V.; Xu, X.; Cheng, A.; Mughal, M. R.; Jo, D. G.; Lathia, J. D.; Siler, D. A.; Chigurupati, S.; Ouyang, X.; Magnus, T.; Camandola, S.; Mattson, M. P. *Proc. Natl. Acad. Sci. U S A* **2007**, *104*, 13798.
8. Kleinert, H.; Schwarz, P. M.; Forstermann, U. *Biol. Chem.* **2003**, *384*, 1343.
9. Diaz-Guerra, M. J.; Velasco, M.; Martin-Sanz, P.; Bosca, L. *J. Biol. Chem.* **1996**, *271*, 30114.
10. Beck, K. F.; Sterzel, R. B. *FEBS Lett.* **1996**, *394*, 263.
11. Jacobs, A. T.; Ignarro, L. J. *J. Biol. Chem.* **2001**, *276*, 47950.
12. Gao, J. J.; Filla, M. B.; Fultz, M. J.; Vogel, S. N.; Russell, S. W.; Murphy, W. J. *J. Immunol.* **1998**, *161*, 4803.
13. Ohmori, Y.; Hamilton, T. A. *J. Leukoc. Biol.* **2001**, *69*, 598.

14. Lee, J. H.; Jung, H. S.; Giang, P. M.; Jin, X.; Lee, S.; Son, P. T.; Lee, D.; Hong, Y. S.; Lee, K.; Lee, J. J. *J. Pharmacol. Exp. Ther.* **2006**, *316*, 271.
15. Yamamoto, T.; Yoshimura, M.; Yamaguchi, F.; Kouchi, T.; Tsuji, R.; Saito, M.; Obata, A.; Kikuchi, M. *Biosci. Biotechnol. Biochem.* **2004**, *68*, 1706.
16. Cheng, Z.; Lin, C.; Hwang, T.; Teng, C. *Biochem. Pharmacol.* **2001**, *61*, 939.
17. Ninomiya, M.; Efdi, M.; Inuzuka, T.; Koketsu, M. *Phytochemistry Lett.* **2010**, *3*, 96.
18. Itoh, T.; Ninomiya, M.; Nozawa, Y.; Koketsu, M. *Bioorg. Med. Chem.* **2010**, *18*, 7052.
19. Chan, E. D.; Riches, D. W. *Am. J. Physiol. Cell Physiol.* **2001**, *280*, C441.
20. Stark, G. R.; Kerr, I. M.; Williams, B. R.; Silverman, R. H.; Schreiber, R. D. *Annu. Rev. Biochem.* **1998**, *67*, 227.
21. Narender, T.; Papi Reddy, K. *Tetrahedron Lett.* **2007**, *48*, 3177.
22. Blackwell, T. S.; Christman, J. W. *Am. J. Respir. Cell Mol. Biol.* **1997**, *17*, 3.
23. Ban, H. S.; Suzuki, K.; Lim, S. S.; Jung, S. H.; Lee, S.; Ji, J.; Lee, H. S.; Lee, Y. S.; Shin, K. H.; Ohuchi, K. *Biochem. Pharmacol.* **2004**, *67*, 1549.
24. Kim, J. Y.; Park, S. J.; Yun, K. J.; Cho, Y. W.; Park, H. J.; Lee, K. T. *Eur. J. Pharmacol.* **2008**, *584*, 175.
25. Ahmad, S.; Israf, D. A.; Lajis, N. H.; Shaari, K.; Mohamed, H.; Wahab, A. A.; Ariffin, K. T.; Hoo, W. Y.; Aziz, N. A.; Kadir, A. A.; Sulaiman, M. R.; Somchit, M. N. *Eur. J. Pharmacol.* **2006**, *538*, 188.
26. Cho, Y. C.; Kim, H. J.; Kim, Y. J.; Lee, K. Y.; Choi, H. J.; Lee, I. S.; Kang, B. Y. *Int. Immunopharmacol.* **2008**, *8*, 567.
27. Falvo, J. V.; Parekh, B. S.; Lin, C. H.; Fraenkel, E.; Maniatis, T. *Mol. Cell Biol.*

2000, 20, 4814.

28. Bach, E. A.; Aguet, M.; Schreiber, R. D. *Annu. Rev. Immunol.* **1997**, 15, 563.
29. Wen, Z.; Zhong, Z.; Darnell, J. E., Jr. *Cell* **1995**, 82, 241.
30. Takaoka, A.; Tanaka, N.; Mitani, Y.; Miyazaki, T.; Fujii, H.; Sato, M.; Kovarik, P.; Decker, T.; Schlessinger, J.; Taniguchi, T. *EMBO J.* **1999**, 18, 2480.
31. Goh, K. C.; Haque, S. J.; Williams, B. R. *EMBO J.* **1999**, 18, 5601.
32. Chang, Y. J.; Holtzman, M. J.; Chen, C. C. *Mol. Pharmacol.* **2004**, 65, 589.
33. Pandey, M. K.; Sung, B.; Ahn, K. S.; Aggarwal, B. B. *Mol. Pharmacol.* **2009**, 75, 525.

Figure legends

Figure 1. LPS induces iNOS mRNA expression in HAPI cells.

(A) Time-course study. HAPI cells were treated with or without LPS (100 ng/mL) for 3, 6, 9, 12 and 24 h. After the treatment, total RNA was extracted, and then RT-PCR was performed. A representative result from three independent experiments is shown. (B) Dose-dependent study. HAPI cells were treated with or without LPS (1, 10, 100 and 1000 ng/mL) for 6 h. After the treatment, total RNA was extracted, and then RT-PCR was performed. A representative result from three independent experiments is shown.

Figure 2. Chemical structure of isolated compounds from *Brassica rapa* L. 'hidabeni'.

Figure 3. Effects of compounds on LPS-induced iNOS and IL-1 β mRNA expression

(A) and NO production (B). (A) HAPI cells were pretreated with each compound (**A1** – **A6**, 50 μ M) for 30 min, followed by treatment with or without LPS (100 ng/mL) for 6 h. Each compound was present 30 min prior to and during LPS treatment. After the treatment, total RNA was extracted, and then RT-PCR was performed. Values (mean \pm SEM, n=3) are expressed as a percentage compared with the mRNA expression level in cells treated with LPS alone. * and **, significant differences ($P < 0.05$ and $P < 0.01$, respectively) compared with cells treated with LPS alone. (B) HAPI cells were pretreated with each compound (**A1** – **A6**, 50 μ M) for 30 min, followed by treatment with or without LPS (100 ng/mL) for 24 h. Each compound was present 30 min prior to and during LPS treatment. Nitrite level in culture medium was measured by the Griess method. Values (mean \pm SD, n=3) are expressed as the fold induction relative to untreated cells. * and **, significant differences ($P < 0.05$ and $P < 0.01$, respectively)

compared with cells treated with LPS alone.

Figure 4. Effect of **A2** on NF- κ B and MAPK pathways.

(A) Effect of **A2** on nuclear translocation of NF- κ B. HAPI cells were pretreated with **A2** (50 μ M) or vehicle for 30 min, followed by treatment with or without LPS (100 ng/mL) for 3 h. Nuclear extracts were prepared from the treated cells, and then subjected to Western blot analysis. A representative blot from three independent experiments is shown. (B) Effect of **A2** on phosphorylation of MAPKs. HAPI cells were pretreated with **A2** (50 μ M) or vehicle for 30 min, followed by treatment with or without LPS (100 ng/mL) for 1 h. Whole cell lysates were prepared from the treated cells, and then subjected to Western blot analysis. A representative blot from three independent experiments is shown.

Figure 5. **A2** suppressed activation of IFN- β signal triggered by LPS.

(A) Effect of compounds on LPS-induced IFN- β mRNA expression. HAPI cells were treated with or without LPS (100 ng/mL) for 6 h. Each compound (**A1** – **A6**, 50 μ M) or vehicle was present 30 min prior to and during LPS treatment. After the treatment, total RNA was extracted, and then RT-PCR was performed. Values (mean \pm SEM, n=3) are expressed as a percentage compared with the mRNA expression level in cells treated with LPS alone. (B) Effect of **A2** on LPS-induced phosphorylation of STAT1. HAPI cells were pretreated with **A2** (50 μ M) or vehicle for 30 min, followed by incubation with or without LPS (100 ng/mL) for 3 h. Whole cell lysates were prepared from the treated cells, and then subjected to Western blot analysis. A representative blot from three independent experiments is shown. (C) Effect of **A2** on LPS-induced nuclear

translocation of STAT1. HAPI cells were pretreated with **A2** (50 μ M) or vehicle for 30 min, followed by incubation with or without LPS (100 ng/mL) for 3 h. Nuclear extracts were prepared from the treated cells, and then subjected to Western blot analysis. A representative blot from three independent experiments is shown.

Figure 6. Effects of synthetic ‘hidabeni’ chalcone derivatives on LPS-induced NO production (A) and iNOS mRNA expression (B). (A) HAPI cells were pretreated with each compound (**A1**, **A2**, **A7** – **A11**, 50 μ M; L-NAME 1 mM) or vehicle for 30 min, followed by treatment with or without LPS (100 ng/mL) for 24 h. Each compound was present 30 min prior to and during LPS treatment. Nitrite level in culture medium was measured by the Griess method. Values (mean \pm SD, n=4) are expressed as the fold induction relative to untreated cells. * and **, significant differences ($P < 0.05$ and $P < 0.01$, respectively) compared with cells treated with LPS alone. L-N, L-NAME. (B) HAPI cells were pretreated with each compound (**A1**, **A2**, **A7** – **A11**, 50 μ M) or vehicle for 30 min, followed by treatment with or without LPS (100 ng/mL) for 6 h. Each compound was present 30 min prior to and during LPS treatment. After the treatment, total RNA was extracted, and then RT-PCR was performed. Values (mean \pm SEM, n=3) are expressed as a percentage compared with the mRNA expression level in cells treated with LPS alone. * and **, significant differences ($P < 0.05$ and $P < 0.01$, respectively) compared with cells treated with LPS alone.

Scheme 1. Synthesis of Chalcone Glycoside Derivatives

Figure 1.

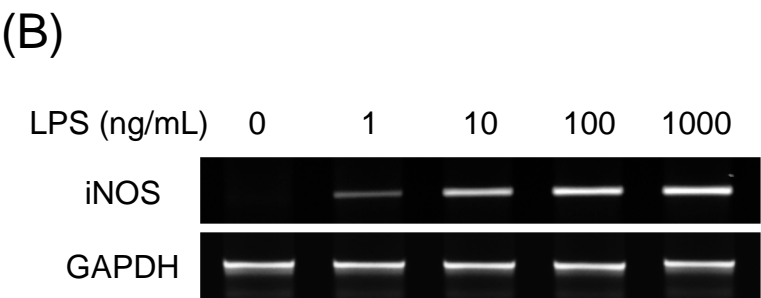
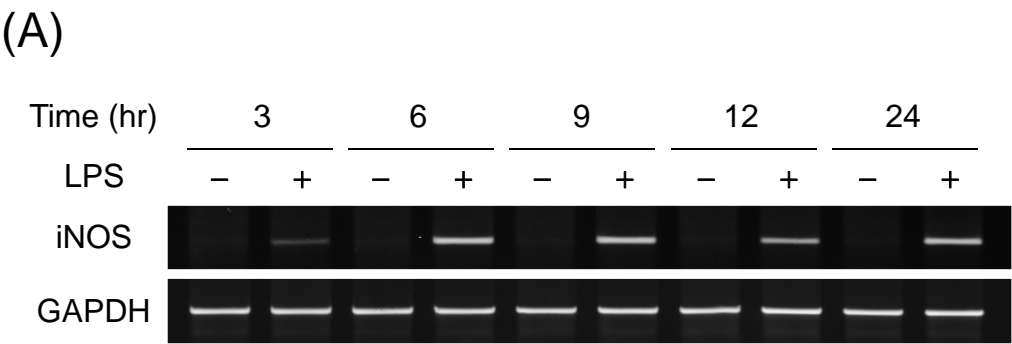
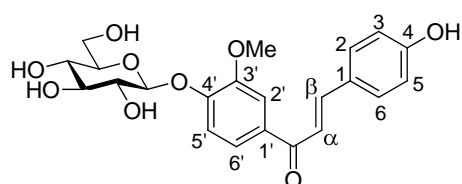
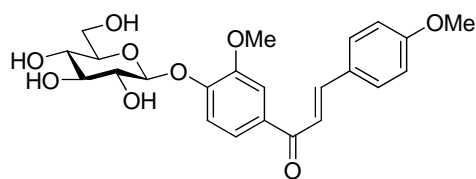


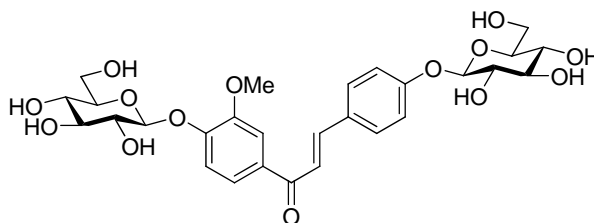
Figure 2.



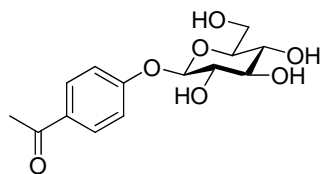
4'-O-β-D-Glucopyranosyl
-4-hydroxy-3'-methoxychalcone (**A1**)



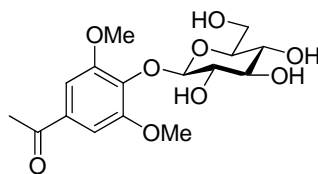
4'-O-β-D-Glucopyranosyl
-3',4-dimethoxychalcone (**A2**)



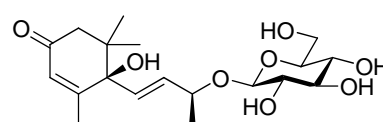
4,4'-Di-O-β-D-glucopyranosyl
-3'-methoxychalcone (**A3**)



Picein (**A4**)



Glucoacetosyringone (**A5**)



Corchoionoside C (**A6**)

Figure 3.

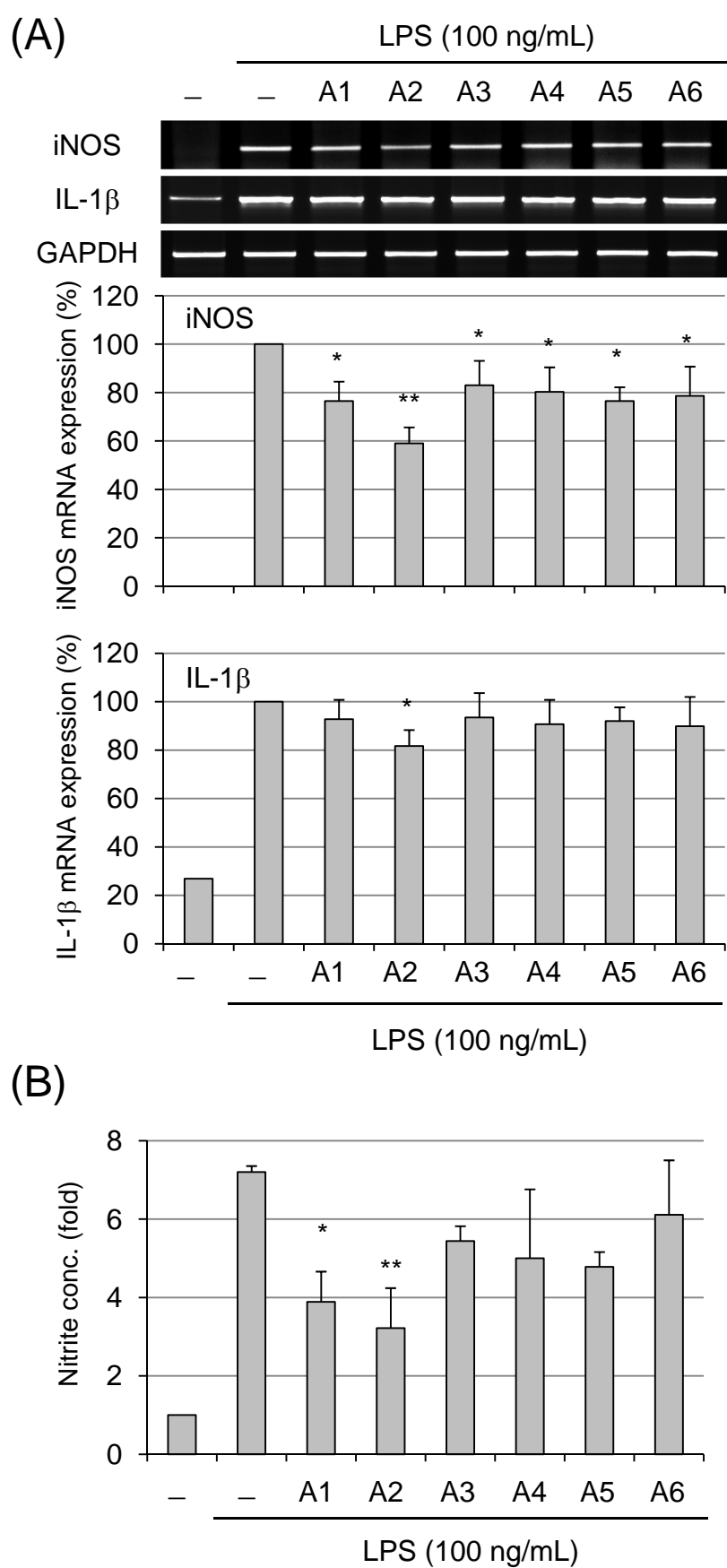


Figure 4.

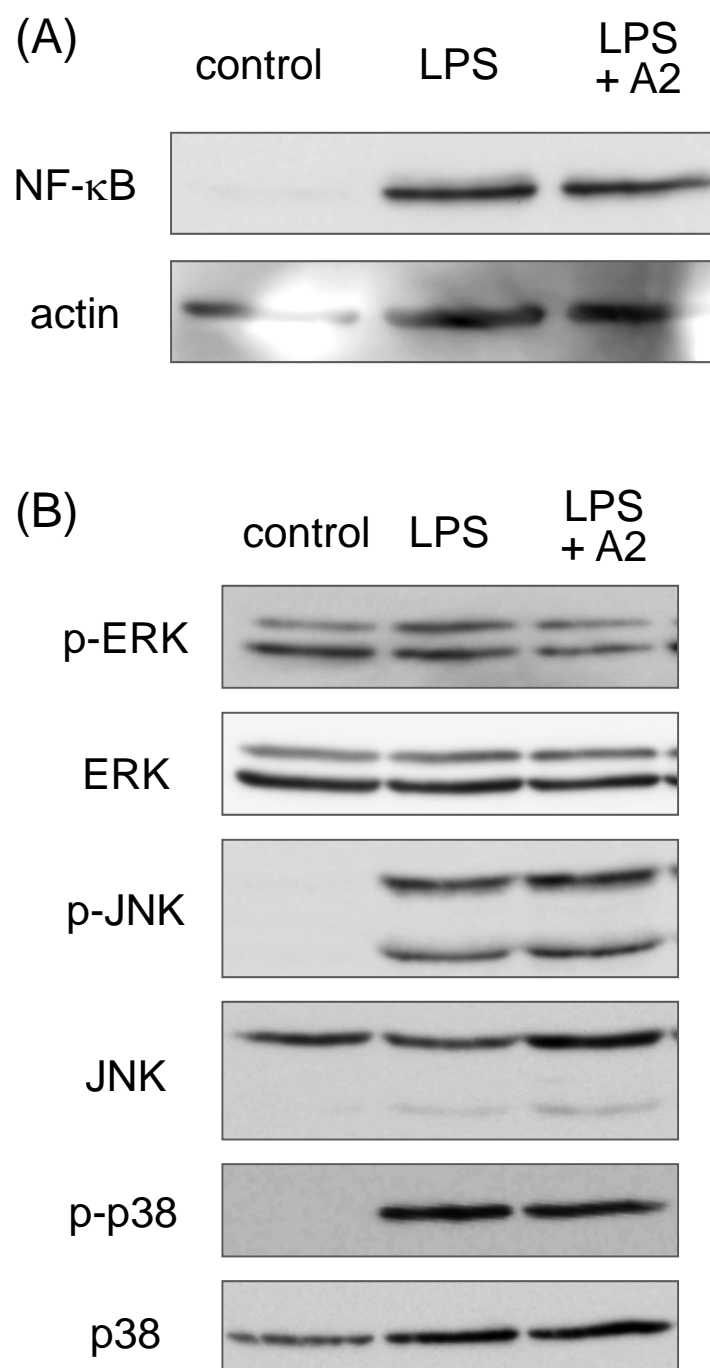


Figure 5.

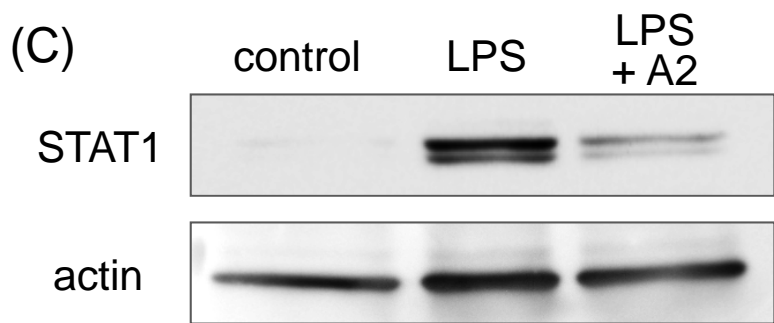
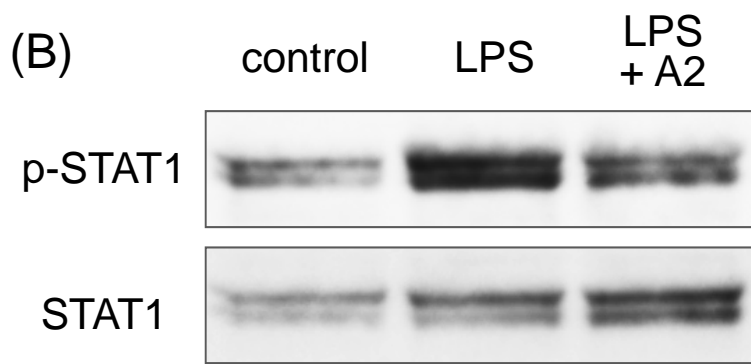
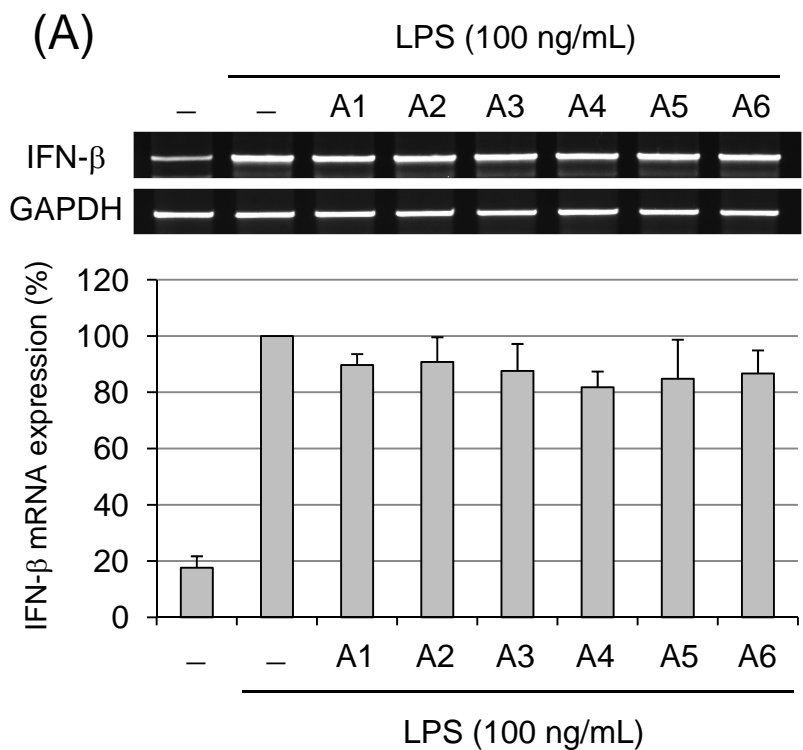
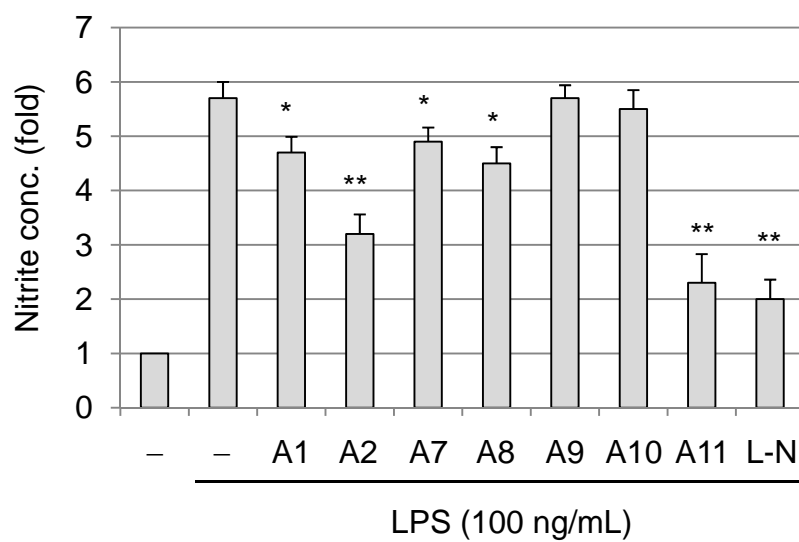
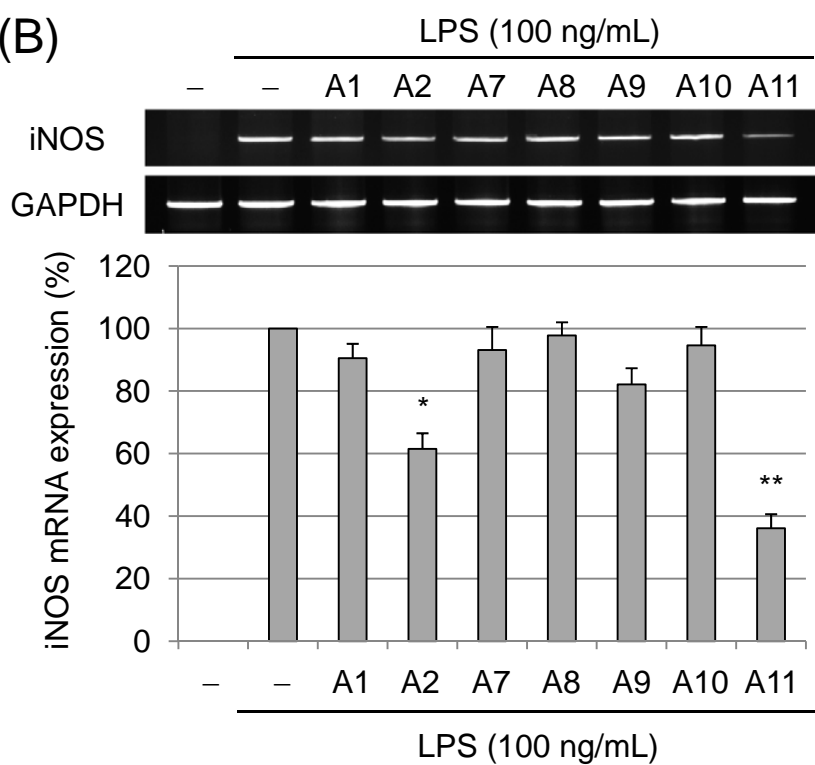


Figure 6.

(A)



(B)



Scheme 1.

